

Solubilities of Mixed Hydroxybenzoic Acid Isomers in Supercritical Carbon Dioxide

Frank P. Lucien* and Neil R. Foster

School of Chemical Engineering and Industrial Chemistry, The University of New South Wales, Sydney 2052, Australia

Studies of the extraction of solid mixtures with supercritical fluids (SCFs) demonstrate that solute–solute interactions in the SCF phase can be significant. To further explore such interactions, the solubilities of various mixtures of hydroxybenzoic acid (HBA) isomers in supercritical CO₂ were determined. Solubility data are reported at pressures ranging from 101 to 203 bar and for temperatures of 318 K and 328 K. Significant solubility enhancements were observed for *m*-HBA and *p*-HBA in systems containing the ortho isomer. The degree of solubility enhancement obtained is possibly the result of hydrogen bonding between the isomers in the SCF phase. The solubility data were correlated with a modified form of the Peng–Robinson equation of state.

Introduction

The solubility of a component in a supercritical fluid (SCF) provides a basic indication of the technical feasibility of any supercritical fluid extraction (SFE) process. For this reason, a considerable amount of solubility data has appeared in the literature (Bartle et al., 1991; Foster et al., 1991). The majority of experimental studies have dealt with binary systems consisting of a single solute, usually a solid, and a single SCF. Solubility data derived from multicomponent systems, in contrast, are relatively scarce.

Since most potential applications of SFE involve the removal of valuable compounds from a matrix of components, binary solubility data present a limited picture of the complex interactions that can occur in the SCF phase. Previous studies involving the extraction of mixtures of solids demonstrate that solute–solute interactions in the SCF phase can be significant (Lucien and Foster, 1996; Iwai et al., 1993; Kurnik and Reid, 1982). In most cases solute–solute interactions lead to an enhancement in the solubilities of components relative to their respective binary systems. As a consequence, there is now a greater need to understand the solubility behavior of such systems.

Solubility enhancement in mixed solute systems usually follows a pattern described by Dobbs and Johnston (1987). They propose that the solubility of a solid in a ternary system will increase, relative to its binary system, in proportion to the solubility of the other solid in the ternary system. This implies that each of the solutes in the SCF phase behaves like an entrainer (or cosolvent). The entrainer effect is commonly encountered in systems that display solid–fluid equilibria. However, when some form of melting occurs in the solid phase, the pattern for solubility enhancement does not conform to the behavior expected from the entrainer effect (Chung and Shing, 1992).

In a previous investigation, the authors measured the solubilities of mixtures of *p*-hydroxybenzoic acid (*p*-HBA) and *o*-HBA in supercritical CO₂ (Lucien and Foster, 1996). These compounds were specifically chosen as model solutes for the purpose of investigating solute–solute interactions between polar solids. Binary solubility data were also

measured so as to quantify the degree of solubility enhancement. The pattern of solubility enhancement for the mixture of *o*-HBA and *p*-HBA (OP system) was well described by the entrainer effect.

In this work, we present further multicomponent solubility data that complete the data set for the solubilities of HBA mixtures in supercritical CO₂. Ternary solubility data are presented for the mixture of *o*-HBA and *m*-HBA (OM system) and for the mixture of *m*-HBA and *p*-HBA (MP system). Binary solubility data for *m*-HBA are provided for the calculation of solubility enhancements. Finally, solubility data for a quaternary system containing all three isomers are also given (OMP system).

Experimental Section

Solubility measurements were performed using a continuous flow apparatus similar to that used in other solubility studies (Macnaughton and Foster, 1994; Gurdial and Foster, 1991). A detailed description of the apparatus and operating procedure has been reported previously (Lucien and Foster, 1996).

Liquid CO₂ was directed from a cylinder into a high-pressure syringe pump where it was compressed to the desired operating pressure. After leaving the pump the pressurized CO₂ entered a preheating coil, which enabled the CO₂ to reach the extraction temperature. The CO₂ then passed into an equilibrium cell that contained the solid mixture. The preheater and equilibrium cell were placed in a constant-temperature water bath where the temperature was maintained to within ± 0.2 K. The saturated CO₂ stream was expanded to atmospheric pressure through a metering valve thereby precipitating the dissolved solute. An in-line filter was placed after the metering valve to trap the precipitated solute.

Prior to commencement of the experiments, the system was purged with low-pressure CO₂. At the commencement of each run, the system was maintained under static conditions for a period of approximately 30 min. This allowed the system to attain equilibrium once all of the valves were opened to pressurize the various sections of the apparatus. The metering valve was then opened, and

Table 1. Source and Purity of Materials

material	source	purity
carbon dioxide	CIG/Liquid Air	99.8% min
<i>o</i> -hydroxybenzoic acid	Sigma	99+%
<i>m</i> -hydroxybenzoic acid	Sigma	99% min
<i>p</i> -hydroxybenzoic acid	Sigma	99% min

at this point the system pressure was maintained to within $\pm 0.5\%$ of the set point.

The solubility of a solute was determined from the mass of solute collected in both the metering valve and filter and from the corresponding volume of CO_2 passed through the apparatus. The volume of CO_2 associated with the precipitated solute was measured with a wet gas meter or a mass flow sensor. Both types of volume measurement devices were calibrated to determine the CO_2 volume to within $\pm 1\%$. Solubility is expressed here as the mole fraction of the solute in the SCF mixture. Individual solubility data points are the average of at least three experimental runs with a relative standard deviation (RSD) of 5% or less. All of the materials used in this work were used as received. The sources and purities of the materials are shown in Table 1.

A 50:50 mol % composition was used in the OM and MP systems, while the OMP system contained one-third of each isomer. Approximately 150 g of each mixture was prepared by weighing out the required amount of each isomer into a container that was then shaken vigorously for at least half an hour. Each mixture was then packed into an equilibrium cell (300 cm^3) in the form of alternate layers of glass wool and the solid mixture. The same mass of solid was used for the solubility experiments on the *m*-HBA binary system.

The solubilities of mixtures of isomers required the additional task of determining the composition of the solid mixture collected in the metering valve and filter. A rinsing procedure was used to remove the solid mixture from the valve and filter. All rinsings were combined into a known volume of sample solution, which was then analyzed using HPLC. Both the total mass of solid mixture as well as its composition were determined from HPLC analysis. Further details on the rinsing procedure and HPLC analysis are given elsewhere (Lucien and Foster, 1996).

For mixtures involving *o*-HBA, the mass of solute collected was also determined gravimetrically. The analytically determined mass was found to be 2–3% less on average than the gravimetrically determined mass. This was considered to be an acceptable error given that the reported solubility points are the average of three measurements with a RSD of 5% or less. In the determination of the solubilities of pure *m*-HBA and the MP mixture, gravimetric determination of the mass of solute collected was not possible because of the very low solubilities of the meta and para isomers. The mass of solute collected in these cases was only determined analytically using the procedure described above.

The suitability of the apparatus for solubility measurement was assessed by measuring the solubility of naphthalene as described in the OP study. Flow rate experiments were also undertaken previously on the *o*-HBA and *p*-HBA binary systems and on the OP mixture to establish the conditions under which equilibrium could be achieved. Flow rates of 12 standard liters per hour (SLPH) or less were used for the experiments on the *m*-HBA binary system. Operating at a flow rate of 5 to 10 L/h was considered sufficient for saturation in the OM, MP, and OMP systems.

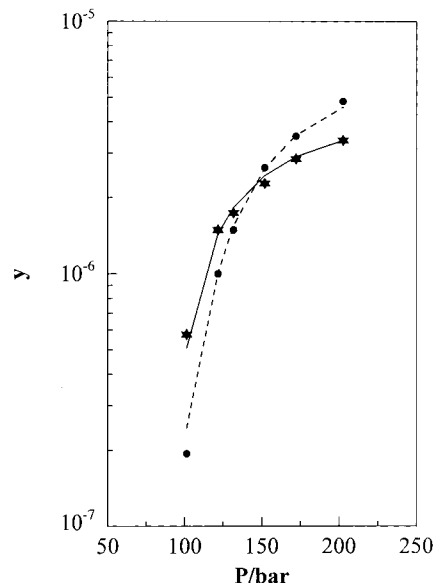


Figure 1. Mole fraction solubility y of *m*-HBA in supercritical CO_2 : (★) 318 K; (●) 328 K. Lines represent correlation of the data with the modified PREOS.

Table 2. Solubility of *m*-HBA in Supercritical CO_2

P/bar	$10^6 y$		P/bar	$10^6 y$	
	$T = 318 \text{ K}$	$T = 328 \text{ K}$		$T = 318 \text{ K}$	$T = 328 \text{ K}$
101.3	0.576	0.194	152.0	2.28	2.63
121.6	1.49	1.00	172.2	2.85	3.50
131.7	1.74	1.49	202.6	3.37	4.81

The phase behavior under supercritical conditions for all HBA systems was checked using a Jerguson sight gauge. Several grams of the solute were placed in a sight gauge, which was then fitted in place of the equilibrium cell. The system was pressurized slowly at 328 K over a period of 2 h to the maximum pressure used in this work and was then held under static conditions for a further hour. No melting point depression was observed in any of the pure and mixed solute systems investigated.

Results and Discussion

Binary Solubility. The measured solubility of *m*-HBA in supercritical CO_2 is listed in Table 2 and shown graphically as a function of pressure in Figure 1. The solubility data for *m*-HBA generally fall in the range of 10^{-7} to 10^{-5} mole fraction. The data for this isomer exhibit the same trends as those for *o*-HBA and *p*-HBA, which reinforces the validity of the experimental method. The relative difference in solubility between the three isomers is illustrated in Figure 2. It is clear from this figure that the completed solubility data set is consistent with the findings of Krukonic and Kurnik (1985), who measured the solubilities at 373 K and for pressures greater than 207 bar.

Solubility data are also commonly related to the density of the pure solvent (Macnaughton et al., 1995; Kumar and Johnston, 1988). A linear relationship normally exists between the logarithm of solubility and solvent density as shown in Figure 3. However, deviation from linearity can be more pronounced at lower solvent density, as seen for the 328 K isotherm. An improved correlation of the data at 328 K was obtained between the logarithm of solubility and the logarithm of solvent density (3.3% AARD).

Ternary Solubility. The solubility data for the HBA isomers in the OM and MP systems are presented in Tables

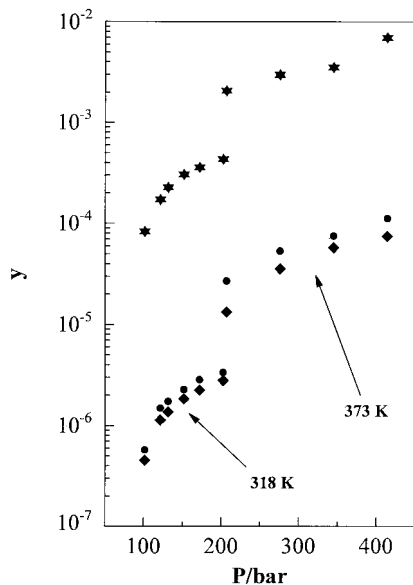


Figure 2. Mole fraction binary solubilities y of the HBA isomers at 318 K and 373 K: (★) *o*-HBA; (●) *m*-HBA; (◆) *p*-HBA. Data at 373 K are from Krukonic and Kurnik (1985).

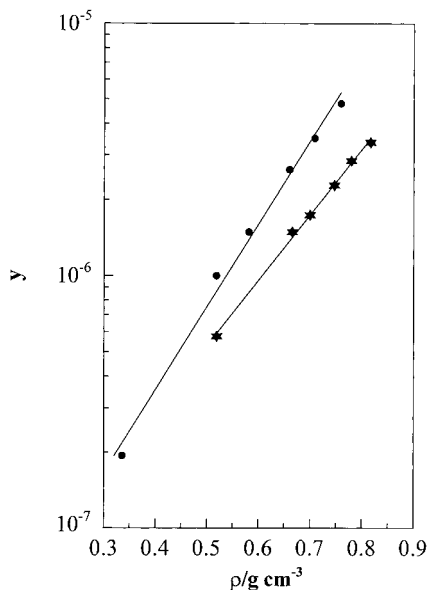


Figure 3. Mole fraction binary solubility y of *m*-HBA as a function of CO_2 density: (★) 318 K; (●) 328 K. Lines represent regression fit of the data: 2.3% AARD and 8.5% AARD at 318 K and 328 K, respectively.

Table 3. Solubility of a 50:50 mol % Mixture of *o*-HBA and *m*-HBA in Supercritical CO_2 at 318 K

P/bar	<i>o</i> -HBA $10^4 y$	solubility enhancement ^a (%)	<i>m</i> -HBA $10^6 y$	solubility enhancement (%)
101.3	0.794	-4	0.968	68
121.6	1.86	8	2.78	87
131.7	2.35	4	3.72	114
152.0	2.93	-4	4.88	115
172.2	3.56	-1	6.20	118
202.6	4.36	1	7.94	136
average		1		106

^a Solubility enhancement is defined as the percent relative deviation of the ternary solubility from the binary solubility of a component at the same temperature and pressure.

3 and 4. Two isotherms (318 K and 328 K) were generated for the MP system, while only one isotherm (318 K) was measured for the OM system. The tabulated results also

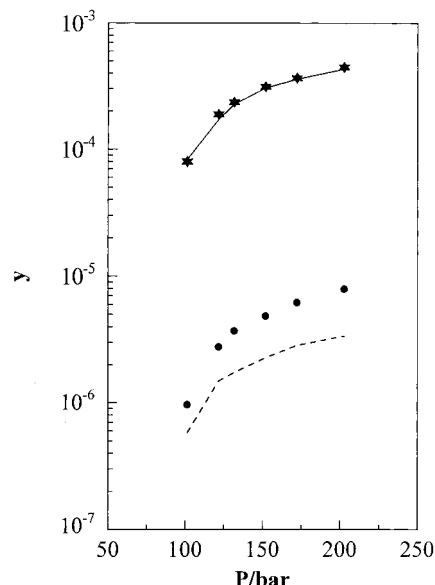


Figure 4. Enhancement of the mole fraction solubility y of *m*-HBA in the OM system at 318 K: (★) *o*-HBA (ternary); (○) *o*-HBA (binary); (●) *m*-HBA (ternary); (---) *m*-HBA (binary).

Table 4. Solubility of a 50:50 mol % Mixture of *m*-HBA and *p*-HBA in Supercritical CO_2

P/bar	<i>m</i> -HBA $10^6 y$	solubility enhancement (%)	<i>p</i> -HBA $10^6 y$	solubility enhancement (%)
$T = 318 \text{ K}$				
101.3	0.595	3	0.450	0
121.6	1.40	-6	1.18	4
131.7	1.72	-1	1.43	4
152.0	2.29	1	1.77	-4
172.2	2.81	-1	2.35	5
202.6	3.23	-4	2.76	-1
average		-1		1
$T = 328 \text{ K}$				
101.3	0.219	13	0.166	17
121.6	1.12	12	0.849	16
131.7	1.63	9	1.22	8
152.0	2.71	3	2.01	6
172.2	3.56	2	2.68	-4
202.6	4.63	-4	3.52	-6
average		6		6

show the corresponding solubility enhancements relative to the binary solubility data. The ternary solubility data were measured at the same pressures used for the binary solubility data so that direct comparisons between the data sets could be made, eliminating the need to interpolate.

To confirm the presence or absence of solubility enhancement, the binary and ternary solubility data sets in this study were compared statistically. The analysis was simplified by considering the average solubility enhancement. For example, at each temperature, the binary and ternary solubilities of a component were determined at six different pressures. An average value for the solubility enhancement was calculated from the six individual values. The average solubility enhancement was then tested statistically to determine whether it differed significantly from zero. The statistical test was only used for those components that had an average solubility enhancement of less than 10%.

The solubility of *m*-HBA, in the presence of *o*-HBA, was enhanced by up to 140%, while no change appears to have occurred in the solubility of *o*-HBA. This result is more clearly demonstrated in Figure 4 and supports the postulate of Dobbs and Johnston (1987) that a more soluble solid

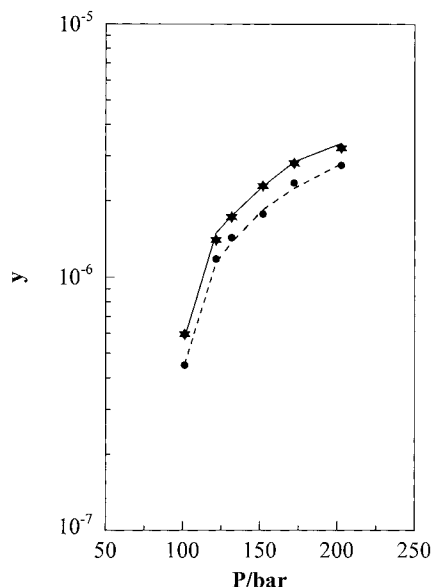


Figure 5. Comparison between binary and ternary mole fraction solubility data y for the MP system at 318 K: (★) *m*-HBA (ternary); (●) *m*-HBA (binary); (●) *p*-HBA (ternary); (- -) *p*-HBA (binary).

causes a more significant increase in the solubility of a less soluble component than vice versa. The negligible enhancement for *o*-HBA was attributed to the extremely low solubility of *m*-HBA. The same type of behavior was observed in the OP system except that the maximum solubility enhancement for *p*-HBA was somewhat higher at 170%.

The solubilities of *m*-HBA and *p*-HBA in the MP system were unchanged from their respective binary values as shown in Figure 5. While the two isomers have comparable solubilities, it would appear that the overall magnitude of the solubility was too low for either isomer to exert any significant influence over the other. The average solubility enhancements for the meta and para isomers at 318 K were -1% and 1%, respectively, which reconfirms the accuracy of the binary solubility data.

The data at 328 K were a little unusual in that larger than normal solubility enhancements in the range of 10–20% were observed for both isomers at the lower pressures. The discrepancies were attributed to errors in the ternary data set, as indicated by the fact that the solubility enhancements for the two isomers follow the same trend. The statistical test for the data at 328 K also confirmed that the average solubility enhancement was not significantly different from zero.

The magnitude of solubility enhancement in the OP and OM systems is considerably greater than that in other mixed solute systems. The general pattern of solubility enhancement in mixed solute systems suggests that negligible enhancement of *p*-HBA and *m*-HBA would be expected for the range of concentration of *o*-HBA ($<10^{-3}$ mole fraction) in the fluid phase (Lucien, 1996). The OP and OM systems reflect the same behavior as the *o*-HBA–aspirin system (Tavana and Randolph, 1991) and demonstrate that a greater potential for solubility enhancement occurs for mixtures of polar solids. The hydrogen-bonding sites present in the HBA isomers suggest that there may be hydrogen bonding occurring between the isomers in the SCF phase.

Quaternary Solubility. The presence of *o*-HBA in the OP and OM systems caused the solubilities of the para and meta isomers to be significantly enhanced relative to their

Table 5. Solubility of an Equimolar Mixture of *o*-HBA, *m*-HBA, and *p*-HBA in Supercritical CO₂ at 318 K

<i>P</i> /bar	<i>o</i> -HBA 10 ⁴ <i>y</i>	<i>m</i> -HBA 10 ⁶ <i>y</i>	<i>p</i> -HBA 10 ⁶ <i>y</i>
101.3	0.800	1.00	0.790
121.6	1.90	2.79	2.36
131.7	2.33	3.54	3.06
152.0	3.05	4.89	4.34
172.2	3.77	6.20	5.55
202.6	4.57	7.99	7.19

Table 6. Solubility Enhancements for the OMP Quaternary System Relative to Binary and Ternary Solubility Data

<i>P</i> /bar	<i>o</i> -HBA (%)	<i>m</i> -HBA (%)	<i>p</i> -HBA (%)
Solubility Enhancement Relative to Binary Solubility Data (<i>T</i> = 318 K)			
101.3	-4	74	75
121.6	10	87	107
131.7	3	103	123
152.0	0	115	136
172.2	5	118	148
202.6	6	137	157
average	3	106	124
Solubility Enhancement Relative to Ternary Solubility Data (<i>T</i> = 318 K) ^a			
101.3		3	-2
121.6		0	-2
131.7		-5	-3
152.0		0	-7
172.2		0	-7
202.6		1	-5
average		0	-4

^a Ternary solubility data refers to the system containing the ortho isomer.

respective binary systems. In both cases, the solubility of *o*-HBA was unaffected because the solubility of the other isomer was too low to exert any significant influence.

In this final part of the experimental study, the solubility of a mixture containing all three isomers was measured to determine whether the presence of the para and meta isomers in combination is enough to enhance the solubility of *o*-HBA. In addition to the study of Bamberger et al. (1988), this is the only other reported study to date of a quaternary system consisting of three solids and a SCF. An additional objective of the experiment was to determine whether the solubilities of *m*-HBA and *p*-HBA are enhanced beyond those observed in their ternary systems containing the ortho isomer. Only one isotherm (318 K) was measured, and the data are presented in Table 5. The solubility enhancements are shown relative to binary and ternary solubility data in Table 6.

The solubility of *o*-HBA relative to its binary system was unchanged, indicating that the combined solubility of the other two isomers was still too low to induce solubility enhancement. The enhancement at 121.6 bar is much higher than the other data points, which is consistent with the assertion made in the OP study that the binary solubility of *o*-HBA at this pressure may have been underestimated. The solubilities for the meta and para isomers were once again enhanced to levels similar to those seen in the OM and OP systems.

The statistical comparison between quaternary and ternary data (OM) for *m*-HBA indicated no significant difference between the data sets. The same comparison for *p*-HBA revealed that the average solubility enhancement was significantly different from zero. The mean value of -4% shown in Table 6 therefore indicates a slightly lower solubility for *p*-HBA relative to its solubility in the OP system. This difference is still within the limits of

Table 7. Physical Properties of the HBA Isomers

physical property	<i>o</i> -HBA	<i>m</i> -HBA	<i>p</i> -HBA
melting point/ $^{\circ}\text{C}^a$	159	201.5–203	214.5–215.5
vapor pressure/bar ^b			
45 $^{\circ}\text{C}$	2.25×10^{-6}	1.73×10^{-8}	1.37×10^{-8}
55 $^{\circ}\text{C}$	6.65×10^{-6}	5.03×10^{-8}	3.76×10^{-8}
molar volume/cm ³ mol ⁻¹ ^a	95.7	94.0	92.4

^a Data from Erickson (1982). ^b Data for *m*-HBA and *p*-HBA are estimated.

experimental reproducibility and is attributed to experimental error rather than an actual change in solubility behavior.

Modeling

The experimental solubility data were modeled with a modified form of the Peng–Robinson equation of state (PREOS). The modeling results from the OP study highlighted the general deficiency of the original PREOS in the correlation of binary solubility data. This deficiency was attributed to the inaccuracies in the estimated critical properties of the solutes, which therefore led to poor estimates of the energy and size parameters.

The properties of the HBA isomers required for the modeling of the solubility data are listed in Table 7. Vapor pressure data for *o*-HBA in the temperature range of 39–59 $^{\circ}\text{C}$ have been measured by de Kruif and van Ginkel (1977) using a combined torsion–weighing effusion apparatus. The vapor pressures reported here are the average of the values obtained by torsion effusion and weighing effusion. Solid densities for the three isomers are given by Erickson (1982), and it is assumed that solid density is essentially independent of temperature within the range of interest in this work. Vapor pressure data for *m*-HBA and *p*-HBA were estimated using the method described in the OP study.

Binary Systems. The modified PREOS involved the fitting of the solute energy and size parameters (a_2 and b_2) to the experimental data with the binary interaction parameter (k_{12}) set to zero. This approach to modeling removes the reliance on the critical properties of the solute and has been described elsewhere (Macnaughton and Foster, 1994; Schmitt and Reid, 1986). The energy parameter is normally a function of temperature, but in this study it was made independent of temperature. The energy and size parameters for CO_2 were estimated in the conventional manner.

Optimized values for the energy and size parameters of *m*-HBA isomer were calculated by minimizing the average absolute relative deviation (AARD) over two isotherms. The AARD is defined as follows

$$\text{AARD} = \frac{1}{N} \sum \frac{|y_{\text{corr}} - y_{\text{exp}}|}{y_{\text{exp}}} \quad (1)$$

where y_{corr} and y_{exp} are the correlated and experimental solubility values, respectively, and N is the number of data points.

The results are presented in Table 8 along with the corresponding values for *o*-HBA and *p*-HBA derived from the OP study. A substantial improvement was made in the correlation of solubility data for *m*-HBA. The original PREOS with conventional mixing rules produced AARDs of 21% ($k_{12} = 0.0460$) and 16% ($k_{12} = 0.0189$) at 318 K and

Table 8. Optimized Energy and Size Parameters from the Modified PREOS

solute	$a_2/\text{Pa m}^6 \text{ mol}^{-2}$	$b_2/\text{m}^3 \text{ mol}^{-1}$	AARD (%)	
			318 K	328 K
<i>o</i> -HBA	9.699	1.594×10^{-4}	5.8	2.4
<i>m</i> -HBA	9.671	1.570×10^{-4}	4.9	6.1
<i>p</i> -HBA	9.462	1.522×10^{-4}	5.2	6.6

Table 9. Optimized Solute–Solute Interaction Parameters for Ternary Solubility Data

ternary system	T/K	k_{23}	AARD (%) (solute 2) ^a	AARD (%) (solute 3) ^a
OM	318	−22.5	5.5	17.9
	328	−28.5	6.1	20.2
OP	318	−24.1	4.4	23.6
	328	−57.4	4.9	5.0

^a Solute 2 refers to the more soluble solute in the ternary system, while solute 3 refers to the less soluble solute.

328 K, respectively. In general, the modeling of these binary systems with density-based correlations is more accurate than the modified PREOS. However, for two or more isotherms, the modified PREOS effectively requires fewer adjustable parameters.

Ternary Systems. The modeling of the ternary systems investigated in this study involved the determination of optimal solute–solute interaction parameters. The solute–solute interaction parameter in each ternary system is k_{23} , where the subscript 2 now refers to the more soluble solute and component 3 is the less soluble solute.

In each ternary system, k_{23} was made a function of temperature while the solute–solvent interaction parameters (k_{12} and k_{13}) were all set to zero. The optimized energy and size parameters, obtained from the binary systems, were used in place of the values estimated with the conventional Peng–Robinson expressions. The optimized value of k_{23} at a given temperature was based on the minimum AARD for two isotherms, one isotherm for each solute present in the ternary system.

The ternary solubility data for *o*-HBA in the OM system were well-correlated as shown in Table 9. The fit of the data was comparable with the correlation of the binary data with the modified PREOS (Table 8). In contrast, the model significantly underestimated most of the ternary solubility data for *m*-HBA as shown in Figure 6. Data points in the low-pressure region, in particular, were underestimated by as much as 40%. A large and negative value for k_{23} was needed in an attempt to account for the solubility enhancements. Similar values for k_{23} were obtained in the OP study (also shown in Table 9) and are indicative of strong interactions between the isomers in the fluid phase. The possibility of hydrogen bonding occurring between the isomers was proposed earlier, and the present results further support this notion.

The correlation results for each isomer in the MP system were comparable with the results for their respective binary systems. At 318 K, a large and positive value for k_{23} was obtained, which reflects very little interaction between *m*-HBA and *p*-HBA. This is consistent with the very low solubilities in the SCF phase, which inhibit any significant solubility enhancement. It was previously concluded that solubility enhancement did not occur in the MP system at 328 K even though higher than normal solubility enhancements (10–20%) were observed in the low-pressure region. The large and negative value of k_{23}

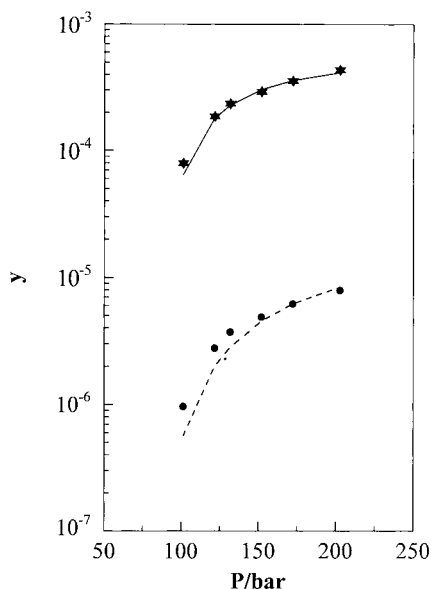


Figure 6. Correlation results from the modified PREOS for the OM system at 318 K: (★) *o*-HBA; (—) *o*-HBA (correlation); (●) *m*-HBA; (- - -) *m*-HBA (correlation).

Table 10. Modeling Results from the Modified PREOS for the OMP Quaternary System

AARD % (ortho)	AARD % (meta)	AARD % (para)
OMP system (overall AARD = 15%)		
5.9	20.2	19.0
binary	OM system ^a	OP system ^a
5.8	17.9	20.2

^a The overall AARDs for the OM and OP systems at 318 K are 11.7% and 13.2%, respectively.

obtained at 328 K is the result of the model accounting for these apparent solubility enhancements.

Quaternary Systems. The three isomers in the quaternary system were assigned the component numbers 2, 3, and 4 in decreasing order of solubility. The conventional mixing rules for this case define three solute–solvent interaction parameters (k_{12} , k_{13} , k_{14}) and three solute–solute interaction parameters (k_{23} , k_{24} , k_{34}). No additional interaction parameters are fitted for the quaternary solubility data because all of the interaction parameters can be obtained from the respective binary and ternary systems. To be consistent with the modeling procedure for ternary systems, all of the solute–solvent interaction parameters were again set to zero. The energy and size parameters for each solute were taken from the modified PREOS results (Table 8).

The individual AARDs for the isomers in the quaternary system are shown in Table 10.

Overall, the modified PREOS produced correlation results that were comparable to those obtained for the ternary systems. This is not a particularly surprising result given that the ternary and quaternary solubility data for each isomer were equivalent. The general deficiency of the model was again highlighted by the underestimation of solubility data in the low-pressure region.

Conclusion

Solubility measurements made on mixtures of HBA isomers in supercritical CO₂ demonstrate the existence of strong solute–solute interactions in the SCF phase. For mixtures containing *o*-HBA, the solubilities of *m*-HBA and *p*-HBA are enhanced in excess of 100% when compared with binary solubility data. The large and negative solute–solute interaction parameters obtained from the modeling of the data are indicative of strong interactions between the isomers in the fluid phase. The modeling results also indicate that manipulation of the solute–solute interaction parameter alone is not sufficient for quantitatively predicting the degree of solubility enhancement observed in these systems.

Literature Cited

- Bamberger, T.; Erickson, J. C.; Cooney, C. L.; Kumar, S. K. Measurement and model prediction of solubilities of pure fatty acids, pure triglycerides, and mixtures of triglycerides in supercritical carbon dioxide. *J. Chem. Eng. Data* **1988**, *33*, 327.
- Bartle, K. D.; Clifford, A. A.; Jafar, S. A.; Shilstone, G. F. Solubilities of solids and liquids of low volatility in supercritical carbon dioxide. *J. Phys. Chem. Ref. Data* **1991**, *20* (4), 713.
- Chung, S. T.; Shing, K. S. Multiphase behavior of binary and ternary systems of heavy aromatic hydrocarbons with supercritical carbon dioxide. *Fluid Phase Equilib.* **1992**, *81*, 321.
- de Kruif, C. G.; van Ginkel, C. H. D. Torsion-weighting effusion vapour-pressure measurements on organic compounds. *J. Chem. Thermodyn.* **1977**, *9*, 725.
- Dobbs, J. M.; Johnston, K. P. Selectivities in pure and mixed supercritical fluid solvents. *Ind. Eng. Chem. Res.* **1987**, *26*, 1476.
- Erickson, S. H. Salicylic acid and related compounds. In *Kirk-Othmer Encyclopedia of Chemical Technology*; Grayson, M., Eckroth, D., Eds.; John Wiley & Sons: New York, 1982; Vol. 20.
- Foster, N. R.; Gurdial, G. S.; Yun, J. S. L.; Liong, K. K.; Tilly, K. D.; Ting, S. S. T.; Singh, H.; Lee, J. H. Significance of the crossover pressure in solid–supercritical fluid equilibria. *Ind. Eng. Chem. Res.* **1991**, *30*, 1955.
- Gurdial, G. S.; Foster, N. R. Solubility of *o*-hydroxybenzoic acid in supercritical carbon dioxide. *Ind. Eng. Chem. Res.* **1991**, *30*, 575.
- Iwai, Y.; Mori, Y.; Hosotani, N.; Higashi, H.; Furuya, T.; Arai, Y.; Yamamoto, K.; Mito, Y. Solubilities of 2,6- and 2,7-dimethylnaphthalenes in supercritical carbon dioxide. *J. Chem. Eng. Data* **1993**, *38*, 509.
- Krukonic, V. J.; Kurnik, R. T. Solubility of solid aromatic isomers in carbon dioxide. *J. Chem. Eng. Data* **1985**, *30*, 247.
- Kumar, S. K.; Johnston, K. P. Modelling the solubility of solids in supercritical fluids with density as the independent variable. *J. Supercrit. Fluids* **1988**, *1*, 15.
- Kurnik, R. T.; Reid, R. C. Solubility of solid mixtures in supercritical fluids. *Fluid Phase Equilib.* **1982**, *8*, 93.
- Lucien, F. P. Ph.D. Thesis, The University of New South Wales, Sydney, Australia, 1996; Chapter 3.
- Lucien, F. P.; Foster, N. R. Influence of matrix composition on the solubility of hydroxybenzoic acid isomers in supercritical carbon dioxide. *Ind. Eng. Chem. Res.* **1996**, *35*, 4686.
- Macnaughton, S. J.; Foster, N. R. Solubility of DDT and 2,4-D in supercritical carbon dioxide and supercritical carbon dioxide saturated with water. *Ind. Eng. Chem. Res.* **1994**, *33*, 2757.
- Macnaughton, S. J.; Kikic, I.; Rovedo, G.; Foster, N. R.; Alessi, P. Solubility of chlorinated pesticides in supercritical carbon dioxide. *J. Chem. Eng. Data* **1995**, *40*, 593.
- Schmitt, W. J.; Reid, R. C. Solubility of monofunctional organic solids in chemically diverse supercritical fluids. *J. Chem. Eng. Data* **1986**, *31*, 204.
- Tavana, A.; Randolph, A. D. Isobaric–isothermal fractional crystallization of organic solids from supercritical fluid mixtures. In *Particle Design via Crystallization*; Ramanarayanan, R., Kern, W., Larson, M., Sikdar, S., Eds.; AIChE Symposium Series, 284; AIChE: New York, 1991; Vol. 87, p 5.

Received for review January 23, 1998. Accepted May 15, 1998.

JE980026U